PROCEEDINGS B

royalsocietypublishing.org/journal/rspb

Research

Cite this article: Ehrlich E, Thygesen UH, Kiørboe T. 2022 Evolution of toxins as a public good in phytoplankton. *Proc. R. Soc. B* **289**: 20220393.
https://doi.org/10.1098/rspb.2022.0393

Received: 28 February 2022
Accepted: 25 May 2022

Subject Category:
Ecology

Subject Areas:
ecology, evolution

Keywords:
toxic algal blooms, evolution of cooperation, coexistence, patchiness in phytoplankton, eco-evolutionary feedback, spatial pattern formation

Author for correspondence:
Elias Ehrlich
e-mail: elias.ehrlich@igb-berlin.de

Electronic supplementary material is available online at https://doi.org/10.6084/m9.figshare.c.6035667.

THE ROYAL SOCIETY PUBLISHING

Evolution of toxins as a public good in phytoplankton

Elias Ehrlich[1,2], Uffe Høgsbro Thygesen[3] and Thomas Kiørboe[4]

[1]Department of Ecology and Ecosystem Modelling, Institute of Biochemistry and Biology, University of Potsdam, Am Neuen Palais 10, 14469 Potsdam, Germany
[2]Department of Fish Biology, Fisheries and Aquaculture, Leibniz Institute of Freshwater Ecology and Inland Fisheries, Müggelseedamm 310, 12587 Berlin, Germany
[3]Department of Applied Mathematics and Computer Science, Technical University of Denmark, 2800 Kongens Lyngby, Denmark
[4]Centre for Ocean Life, DTU Aqua, Technical University of Denmark, 2800 Kongens Lyngby, Denmark

EE, 0000-0003-3610-8200; UHT, 0000-0002-4311-6324; TK, 0000-0002-3265-336X

Toxic phytoplankton blooms have increased in many waterbodies worldwide with well-known negative impacts on human health, fisheries and ecosystems. However, why and how phytoplankton evolved toxin production is still a puzzling question, given that the producer that pays the costs often shares the benefit with other competing algae and thus provides toxins as a 'public good' (e.g. damaging a common competitor or predator). Furthermore, blooming phytoplankton species often show a high intraspecific variation in toxicity and we lack an understanding of what drives the dynamics of coexisting toxic and non-toxic genotypes. Here, by using an individual-based two-dimensional model, we show that small-scale patchiness of phytoplankton strains caused by demography can explain toxin evolution in phytoplankton with low motility and the maintenance of genetic diversity within their blooms. This patchiness vanishes for phytoplankton with high diffusive motility, suggesting different evolutionary pathways for different phytoplankton groups. In conclusion, our study reveals that small-scale spatial heterogeneity, generated by cell division and counteracted by diffusive cell motility and turbulence, can crucially affect toxin evolution and eco-evolutionary dynamics in toxic phytoplankton species. This contributes to a better understanding of conditions favouring toxin production and the evolution of public goods in asexually reproducing organisms in general.

1. Introduction

Toxic phytoplankton blooms are a global phenomenon and pose a threat to human health, strongly affect ecosystem functions, and may cause substantial economical losses in fishery, aquaculture, tourism and drinking water supply [1]. A variety of phytoplankton species from different taxonomic groups are able to produce toxins, including marine dinoflagellates, haptophytes, diatoms and freshwater cyanobacteria. These phycotoxins represent all kind of secondary metabolites with diverse biological functions that harm certain organisms of the food web. Blooms of toxic phytoplankton species often show a high intraspecific variation in toxicity, that is, coexisting genotypes with different degrees of toxicity that regulate the harmfulness of the bloom [2,3].

Despite the well-known ecological and economical impact of toxic phytoplankton blooms, we still lack an understanding of how phytoplankton organisms have evolved toxin production and what drives the often observed maintenance of intraspecific variation in toxicity within such blooms. Such an understanding would help in anticipating favourable conditions for toxic phytoplankton blooms and developing management strategies. Research over the past decades has identified a large diversity of phytoplankton toxins [1] and has suggested multiple advantages for their producers. These benefits include

inhibition of competing algae, defence against grazers [4] or parasites [5], toxin-assisted predation in mixotrophs [6], sequestration of redundant nutrients [7], or protection against oxidative stress [8]. Some toxins function as grazer deterrents, reducing the risk that individual toxin-containing cells are consumed by a zooplankton grazer [9]. Such toxins are 'private goods' and their evolution is easily understood. However, other toxins are not only beneficial to the producing phytoplankton cell but also to non-toxic cells, for example, when the toxin reduces grazing activity from a shared predator or hampers a common competitor. Such toxins constitute a 'public good' [4]. This holds especially for extracellular phytoplankton toxins that diffuse in water and sheer off from their producers [10]. Toxins released by terrestrial plants, by contrast, represent a more exclusive good, as they stay close to the producing plant [11].

The evolution of toxin production as a public good in phytoplankton is difficult to explain, given that its costs are payed 'privately' by the producing strain [12]. General theory on public goods predicts that they can evolve if they favour the cooperators (i.e. the altruistic strain paying the costs) more than the cheaters (i.e. another strain of the same species or other species that benefit but do not pay the cost) [10,13]. However, many toxins leak out of cells, are actively secreted, or become available after cell lysis [6,14], which spreads the benefit also to non-toxic cells. Even intracellular toxins could be similarly beneficial to the non-toxic competitors, for example, when the consumption of toxic cells reduces the predators' further feeding activity [9]. Hence, under the traditional assumption that phytoplankton live in a homogeneous environment, toxins would favour toxic and non-toxic cells equally.

Small-scale spatial heterogeneity in cell distribution may allow toxic cells to share the advantage more with nearby conspecifics than with distant non-toxic ones. This would allow for positive kin selection of the toxic strain [15]. Spatial heterogeneity in phytoplankton has traditionally been observed on larger scales of kilometres [16], but current research provides empirical evidence that patchiness occurs also on small scales down to millimetres [17]. Young *et al.* [18] showed that such small-scale patchiness of organisms may simply result from cell death and asexual reproduction via binary division, which is common in phytoplankton, and is maintained even in a turbulent environment.

Here, we examine whether demographic processes can provide the critical spatial heterogeneity needed for the evolution of toxic phytoplankton and explore under which conditions it holds. Furthermore, we consider the long-term dynamics of toxic and non-toxic genotypes within a phytoplankton species. In contrast to traditional phytoplankton models, which typically ignore small-scale spatial heterogeneity, we use an individual-based model considering phytoplankton cells randomly reproducing, dying, moving (diffusing), producing toxins and competing for nutrients in a two-dimensional space. In our model, we refer to toxins as a public defense against grazing, but our results also provide general implications for toxins with other public benefits.

2. Methods

Our individual-based model is based on the Brownian bug model of Young *et al.* [18], but includes three important extensions: (i) genetic diversity, that is, phytoplankton cells belong either to a toxic or a non-toxic strain; (ii) toxin production; and (iii) nutrient competition. We consider extracellular toxins that leak out of toxic cells, diffuse and decay. High toxin concentrations locally reduce the mortality of both strains. This mimics here a defense against predation without implementing an explicit zooplankton grazer, but can be interpreted in a broader sense as a general fitness increase by toxins. The degree to which toxins are a private or public good depends on their distribution and the presence of other cells around the producing cells (electronic supplementary material, figure S2). We assume that toxin production is non-inducible and comes at the cost of a lower cell division rate. The model code was written in Julia and is available under https://github.com/ehrlichehrlich/ToxicAlgaeEvol.

The model simulations run for 12 000 days in discrete time steps dt of 2 h. Each simulation step consists of four consecutive processes: (1) Cell division and nutrient consumption. (2) Death and nutrient recycling. (3) Toxin leakage and decay. (4) Cell movement and diffusion of nutrients and toxins. We track the positions of all individual phytoplankton cells in a $L \times L$ square ($L = 50$ cm), which is divided into grid cells of size d$x = 0.5$ cm and has periodic boundary conditions. Further state variables are the nutrient and toxin concentration at each grid cell.

For the standard run, at $t = 0$, we randomly and independently place 10^4 non-toxic cells into the simulation space. Toxic cells and toxins are initially absent. The nutrients are initially homogeneously distributed with a concentration N_I, referring to typical nitrate concentrations found in the ocean. After 1000 simulation days, when the non-toxic resident community has settled, we randomly replace 100 non-toxic cells by toxic ones, mimicking the invasion event (i.e. emergence of toxin mutation). In the sensitivity analysis, we start the simulations with both strains initially present at a random distribution (9×10^3 non-toxic and 10^3 toxic cells), as the non-toxic strain does not survive alone for several parameter combinations and the focus is more on the long-term dynamics and the maintenance of intraspecific variation in toxicity.

(a) Cell division and nutrient consumption

Cells reproduce via binary division with probability $R = e^{r\,dt} - 1$, where the 'offspring' cells emerge at the same place as the 'parental' one [18]. We derive R from the growth rate $r = r_{max}(N/(H_N + N))$, which depends on the local nutrient concentration N, the maximum growth rate r_{max} and the half-saturation constant for nutrient uptake H_N. Cell division requires uptake of nutrients given by the cell quota q_N. Due to time discreteness, negative nutrient concentrations may occur at grid cells where the reproducing phytoplankton cells A_{rep} would consume more nutrients than available at that location, i.e. $A_{rep}\,q_N > N$. To avoid this, we consecutively pick random cells from that location and undo their reproduction until $A_{rep}\,q_N \leq N$.

(b) Toxins, cell death and nutrient recycling

Toxins leak out of toxic cells at rate Q and decay at rate λ, given their lability in water. The death probability of a cell equals the sum of its non-grazing (M) and grazing (G) mortality (i.e. the fitness component affected by toxins), $M = 1 - e^{-m\,dt}$ and $G = 1 - e^{-g\,dt}$. We assume a constant non-grazing mortality rate m. The grazing mortality rate g depends on the local toxin concentration T, given by $g = g_{max}(1 - (T/(H_T + T)))$. g_{max} is the maximum grazing mortality rate and H_T the half-saturation constant for the toxin effect. Nutrients from dead phytoplankton cells are uniformly released to the whole space, mimicking the effect of grazers that redistribute nutrients from consumed phytoplankton.

(c) Cell movement and molecule diffusion

Like Young *et al.* [18], we model the movement of individual cells as a random walk described by $x(t + dt) = x(t) + \delta x$ and $y(t + dt) =$

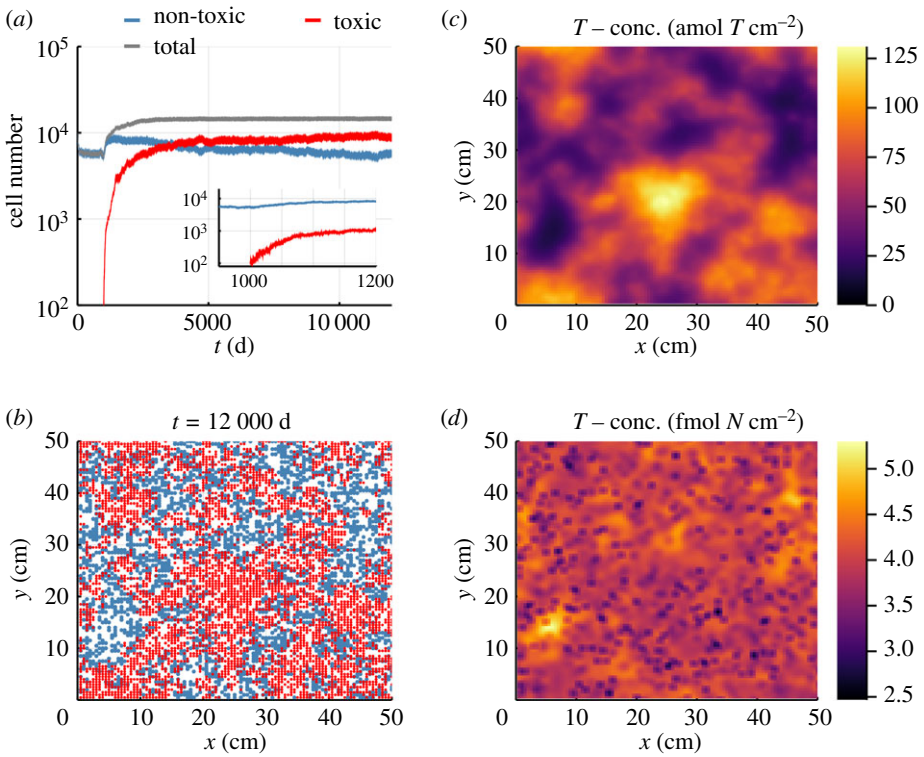

Figure 1. Simulation run with standard parametrization. (*a*) Population dynamics of the two cell genotypes. The embedded small panel zooms into the initial invasion phase of the toxic cells into a resident community of the non-toxic cells. (*b*) Spatial distribution of cells at the end of the simulation, i.e. after 12 000 days, within the 100 × 100 grid. Toxic cells (red in the online version) are printed on top of non-toxic cells (blue in the online version) and partly cover them in the visualization (the dots representing toxic cells are slightly smaller compared to the dots for non-toxic cells). (*c*) Final toxin and (*d*) nutrient distributions. (Online version in colour.)

$y(t) + \delta y$, where x and y refer to the spatial coordinates of the focal cell. δx and δy are independent, Gaussian distributed random variables with a standard deviation of $\sigma = \sqrt{D_C\, 2\, dt}$, corresponding to a cell diffusivity D_C (a surrogate for cell motility).

Diffusion of nutrients and toxins is implemented with standard and simple methods for numerical solution of partial differential equations. Specifically, at each time step, we redistribute the material in a given grid cell over itself and its eight neighbouring grid cells, corresponding to an explicit Euler method using the standard nine-point stencil for the diffusion operator. The diffusivity D is assumed to be equal for both types of molecules, but differs from the diffusivity of cells (D_C) that have a different size and can actively move.

(d) Parametrization

We refer the standard parameter values mainly to a marine dinoflagellate (electronic supplementary material, table S1). In the sensitivity analysis, we explore a broad range of parameter values, accounting for high trait variation among different toxic phytoplankton species (e.g. motility) and for lacking data (e.g. toxin leakage rates). We assume low costs of toxin production, that is, only a slightly reduced r_{max} of toxic compared to non-toxic cells. All other parameter values (m, g_{max}, H_T, H_N, q_N, D_C) are equal for both strains. Due to the two-dimensionality of the model, we convert literature cell or molecule concentrations from three dimensions to two dimensions by keeping the inter-particle distance constant (see electronic supplementary material).

(e) Model runs and output

We first test in a standard scenario without turbulence (electronic supplementary material, table S1) whether a mutant toxic strain can invade a resident community of the non-toxic strain and evaluate the long-term dynamics. A successful invasion implies that toxin evolution is possible. In a sensitivity analysis, we next find the phytoplankton trait values and environmental conditions that allow long-term maintenance of intraspecific variation in toxicity, i.e. coexistence of toxic and non-toxic genotypes. In the electronic supplementary material, figures S3–S6, we demonstrate that our results hold also under turbulence and in three-dimensional space (electronic supplementary material, figures S7 and S8). We run each simulation of the individual-based phytoplankton model for 12 000 days. All output measures (cell numbers, toxin concentrations, correlation coefficients, mean crowding) provided in the following represent means of the last 2000 simulation days, averaged across 10 replicates.

3. Results

(a) Invasion success and long-term model behaviour

In the standard run, the toxic strain invades and surpasses the cell number of the non-toxic resident (figure 1*a*). Both strains coexist in the long term and show compensatory dynamics, causing a rather constant total cell number (figure 1*a*). This total cell number reaches higher values than in the purely non-toxic resident community (figure 1*a*), as toxins reduce the grazing losses and thus increase the steady-state concentration.

Both strains show strong patchiness and are separated in space (figure 1*b*). The low overlap between non-toxic and toxic patches results in a negative spatial correlation of their cell numbers (Pearson's correlation coefficient $\rho = -0.17$). In patches of toxic cells, toxin concentrations reach the highest values (figure 1*b*,*c*). Non-toxic cells experience on average lower toxin concentrations ($\bar{T}_{non} = 13\,\text{amol}\,T\,\text{cm}^{-2}$) than toxic ones ($\bar{T}_{tox} = 19\,\text{amol}\,T\,\text{cm}^{-2}$), which explains the success of the latter. Toxin concentration is negatively correlated with nutrient concentration ($\rho = -0.36$), as nutrient exploitation is higher at locations of low mortality (figure 1*c*,*d*).

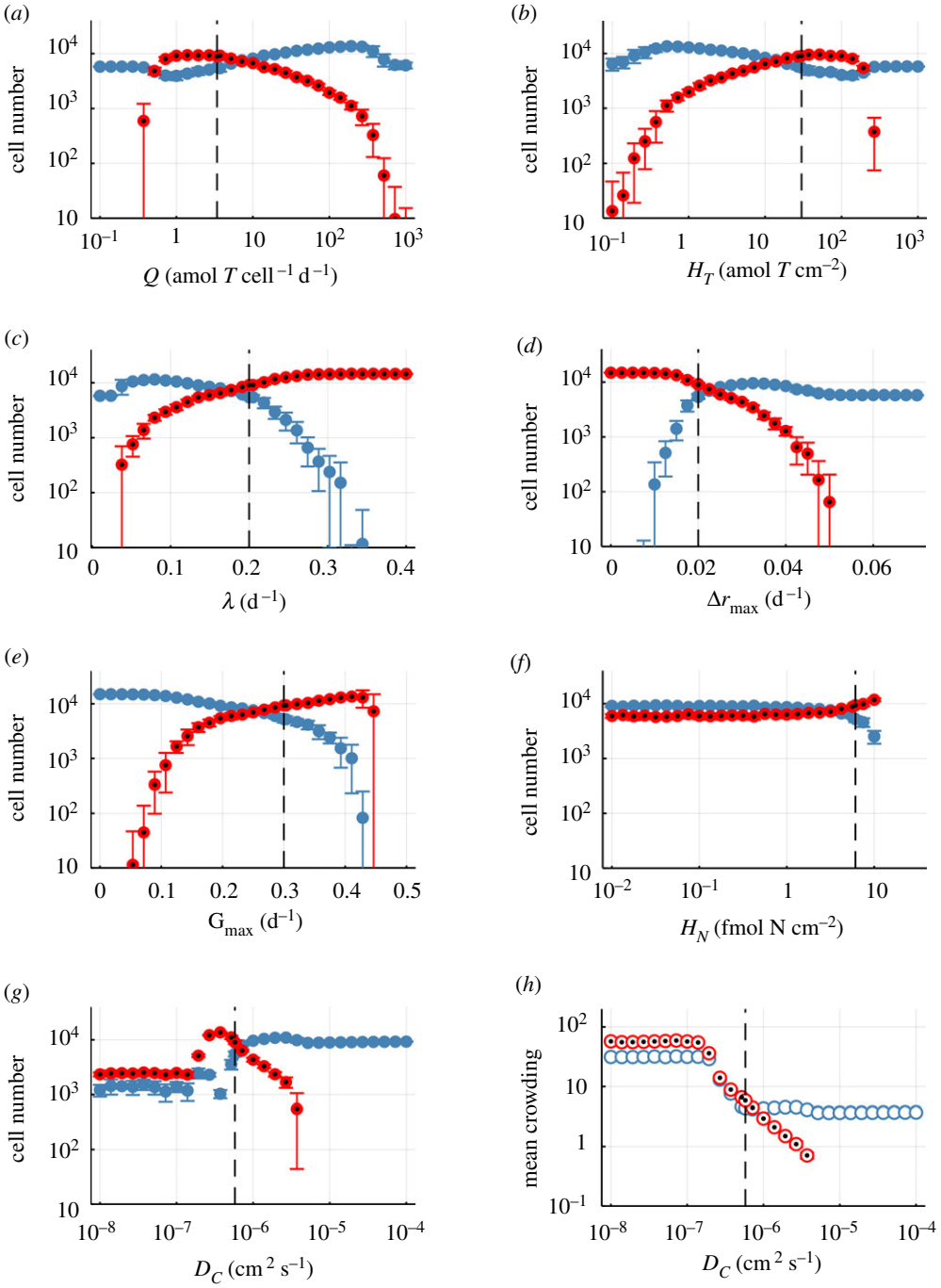

Figure 2. Summary of sensitivity analysis with one parameter changed at a time and all others kept at their standard values. (*a–h*) Mean values and standard deviations for ten replicates of simulations, respectively. (*a–g*) Average total number of toxic (red circles with black dots) and non-toxic cells (blue circles), depending on the toxin leakage rate Q, the half-saturation constant for the toxin effect H_T, the toxin decay rate λ, the costs of toxin production Δr_{max}, the maximum grazing rate G_{max}, the half-saturation constant for nutrient uptake H_N and the diffusivity of cells D_C (motility). The vertical, dashed lines indicate the standard parameter values. Panel (*h*) shows additionally the mean crowding of each strain for different values of D_C. For calculating the crowding, we divided the whole space into quadrats of 1 cm^2 and then counted, for each cell, the number of other cells from the same strain located at the same quadrat [19]. (Online version in colour.)

When putting 'offspring' cells at random (instead of 'parental') places, but keeping the model otherwise the same, patchiness vanishes and toxic cells go extinct quickly (electronic supplementary material, figure S1). This highlights that local reproduction, via binary division, is the key to patchiness and spatial strain separation, on which the invasion and survival of toxic cells as well as the coexistence with non-toxic cells rely.

(b) Sensitivity analysis

Three main principles are important for understanding the following results: (1) If grazing losses are (almost) equal for both strains, non-toxic cells will always outcompete toxic ones due to their higher cell division rate. (2) Grazing losses of the non-toxic and toxic cells converge if they face equal local toxin concentrations, or if toxins become so concentrated that they everywhere exceed the saturation concentration for toxic effects on the grazer (see §2). (3) Patchiness and spatial strain separation generated by binary division counteract homogenization of toxin concentrations.

At very high toxin leakage rate, Q, the toxin concentration, everywhere becomes high enough to yield maximum grazing protection (electronic supplementary material, figure S2), even if local toxin concentrations differ

(see (2)). The consequent lack of advantages to toxin production drives the toxic cells to extinction (see (1), figure 2*a*). At very low toxin leakage rate, toxin production is also not warranted, and the toxic strain goes extinct. Only intermediate toxin leakage rates allow the maintenance of the toxic strain (figure 2*a*). The effect of varying the toxin half-saturation constant, H_T, is equivalent but opposite (figure 2*b*). When grazing reduction saturates at a low toxin concentrations, the toxin concentration is everywhere sufficiently high to provide maximum protection, and conversely, at a very high H_T, the toxin concentration is everywhere too low to yield protection (electronic supplementary material, figure S2).

If toxins decay very slowly (low λ), they also reach high concentrations far from the toxic cells (electronic supplementary material, figure S2). Hence, the public good is widely shared with neighbouring non-toxic cells, sealing the extinction of the toxic strain (figure 2*c*). With increasing toxic decay rate, the toxins become increasingly 'private', with high concentrations only near toxic cells. The density of toxic cells increases, while the non-toxic cells decrease until they go extinct at very high decay rates (figure 2*c*).

The cost of toxin production (Δr_{max}) is defined as the difference between the maximum growth rate of non-toxic ($r_{max,non} = 0.7\ d^{-1}$) and toxic cells ($r_{max,\ tox}$). The latter one is varied to alter the costs. In the absence of costs, i.e. $\Delta r_{max} = 0.0\ d^{-1}$ (i.e. $r_{max,tox} = 0.7\ d^{-1}$), the toxic cells outcompete non-toxic ones, as expected (figure 2*d*). This holds also for very low costs. With increasing costs, the number of toxic cells decreases, while non-toxic ones enter the system and progressively increase in density (figure 2*d*). When $\Delta r_{max} > 0.05\ d^{-1}$ (i.e. $r_{max,tox} < 0.65\ d^{-1}$), the toxic strain goes extinct and the non-toxic one drops in density to its monoculture level (figure 2*d*).

At a very low grazing pressure (G_{max} close to zero), the toxic cells cannot persist (figure 2*e*). With increasing grazing pressure, toxic cells increase while non-toxic ones decrease in abundance. At a very high grazing pressure, first the non-toxic cells die out ($G_{max} > 0.43\ d^{-1}$) and then also the toxic ones ($G_{max} > 0.45\ d^{-1}$), which finally cannot resist despite their defense (figure 2*e*).

Increasing the half-saturation constant for nutrient uptake H_N is equivalent to decreasing nutrient affinity ($\alpha_i \propto r_{max,i}/H_N$) in our model. The numbers of non-toxic and toxic cells are rather unaffected for a wide range of values of H_N (figure 2*f*). Only above a value of ~1 fmol N cm^{-2} does the toxic strain become increasingly abundant, while the non-toxic cells decrease in number (figure 2*f*). A high H_N implies that cell reproduction can compensate the losses only at high nutrient concentrations. Hence, patches of non-toxic cells are only thinly populated, leading to less likely overlaps with toxic patches. This favours toxic cells, which can exclusively reduce the mortality rate and show higher patch densities with lower nutrient concentrations. At very high H_N values (greater than 10 fmol N cm^{-2}), both strains go extinct as even the toxic strain cannot compensate the grazing losses anymore (figure 2*f*).

The cell diffusivity D_C is a surrogate for cell motility in our model. If D_C is relatively high (greater than $7 \times 10^{-6}\ cm^2\ s^{-1}$), toxic cells die out (figure 2*g*) as high cell motility prevents patchiness (figure 2*h*, low mean crowding) and thus spatial strain separation, which is crucial to the survival of toxic cells. With decreasing D_C, patchiness increases (figure 2*h*). This allows toxic cells to survive and show higher cell numbers, while non-toxic cells first slightly increase and then decline in number (figure 2*g*). After going below an optimum of D_C ($3.7 \times 10^{-7}\ cm^2\ s^{-1}$), the toxic cell number decreases and non-toxic cells become more abundant. Finally, for a low D_C (greater than $1.4 \times 10^{-7}\ cm^2\ s^{-1}$), the densities stay constant for both strains with the toxic one dominating the system (figure 2*g*). The fact that the system does not react any more to changing D_C values relies on the model's discreteness in space. The model grid cell size of 5 mm means that cells only move, if their movement distance along one spatial axis is above 2.5 mm. Very low motility implies that cells basically stay at their place of birth (i.e. after cell division). This keeps strains from occupying more space and thus prevents competitive exclusion.

4. Discussion

Our study illustrates that the evolution of toxins as a public good and coexistence of toxic and non-toxic strains within phytoplankton blooms is possible due to patchiness and spatial strain separation generated by binary division. Low costs and a high fitness increase resulting from toxin production promote toxic strains. We considered toxins as a public defense against grazing, i.e. the fitness increase was high under high grazing pressure. However, the found spatial patterns may also more generally explain dynamics of toxins providing other public benefits (e.g. hampering growth of another phytoplankton species or protection against parasites). We found that selection would favour labile toxins that optimally decay before reaching competing non-toxic strains. For two traits—the toxin leakage rate and effectiveness of toxins in reducing predation losses—we found an optimum curve with the highest densities of the toxic strain occurring at intermediate trait values. A high random (diffusive) cell motility is critical to our results as it destroys patchiness and prevents toxin evolution.

In our standard model the water was static, whereas natural waterbodies exhibit turbulent eddies of different sizes. Including random advection like Young *et al.* [18] to mimic a simple turbulent environment at the cm-scale (near the lowest size scale of turbulence, i.e. the Kolmogorov scale) stretches the patches [18] but does not qualitatively alter our results at low turbulence (electronic supplementary material, figures S3 and S4). However, toxic cells show lower densities than under no turbulence (figure 1; electronic supplementary material, figure S4). With increasing turbulence, the toxic strain is driven towards extinction, but its resistance against turbulence increases with higher toxin decay rates (electronic supplementary material, figures S5 and S6) by narrowing the toxin distributions around the producers. For computational reasons, our model is run in two spatial dimensions. Adding a third dimension to the model leads qualitatively to the same result for the evolution and maintenance of toxicity (electronic supplementary material, figures S7 and S8).

Jonsson *et al.* [20] calculated that turbulence conditions in the open oceans would break up clonal patches, as typical rates of phytoplankton reproduction (the driving force of patchiness) are insufficient to counteract high turbulence dissipation rates. However, Franks *et al.* [21] recently showed that turbulence in the ocean is highly intermittent and most

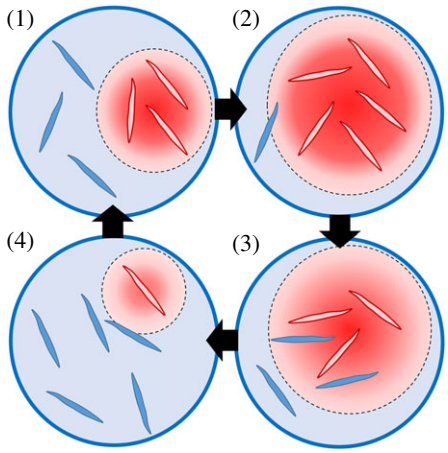

Figure 3. Conceptual visualization of the internal feedback mechanism, allowing for the coexistence of the non-toxic (blue in online version) and toxic strain (red in online version). The reddish areas (with dashed borders) indicate the presence of toxins, where a dark red refers to a high toxin concentration. (Online version in colour.)

of the time very much lower than 'bulk' turbulent dissipation rates. Toxic phytoplankton blooms often occur during summer when turbulence is usually low due to stratification. Furthermore, waterbodies show a high heterogeneity in turbulence [22] and toxic blooms frequently occur in thin subsurface layers of minimal turbulence, e.g. near the pycnocline [23], where they can reduce predator activity [24].

Our model findings are consistent with the frequently observed variation in toxin content among different genotypes sampled from the same location [2,3]. Previous studies surmised that this variation may arise from a lacking strong selection pressure on toxin production [25] and excluded kin selection as an explanation for the success of toxic phytoplankton, as it would only work in monoclonal populations [3]. Our results suggest an alternative interpretation: that stabilizing mechanisms allow for the coexistence of toxic and non-toxic strains and that kin selection is plausible, given the intrinsically generated spatial strain separation.

The stabilizing mechanisms, which form the basis for strain coexistence, can be illustrated by an internal feedback loop (figure 3). (1) Given spatial separation of the two strains, the toxic cells increase in abundance and locally elevate toxin concentration. The resulting lower mortality allows them to exploit nutrients more than neighbouring non-toxic cells that decrease in abundance. (2) At higher abundances of toxic cells, toxins get increasingly concentrated also in areas surrounding the patch of toxic cells. (3) This spreads the public good to non-toxic cells as well, and enables their return. They increase in density in nearby toxic patches, enhancing the spatial overlap of the two strains. At similar levels of toxin concentration in those overlapping regions, non-toxic cells are superior compared to toxic cells and supersede them. (4) At low abundances of the toxic strain, toxins decrease in concentration and become only locally available to toxic cells. The spatial separation of the two strains increases due to the low nutrient availability in the former overlapping regions of high cell densities, where non-toxic cells now decrease. This puts the system back to state (1) and completes the feedback loop. This feedback loop (figure 3) depicts an eco-evolutionary feedback similar to the one described by Driscoll *et al.* [4], but with more emphasis on the importance of the spatial population structure. Furthermore, step 3 of the feedback loop illustrates that the inverse evolutionary path is also possible, i.e. a non-toxic genotype emerges in a toxic population, as indicated by empirical studies [3,26].

In our model, we assumed that the phytoplankton cells produce toxins at a fixed rate. In nature, many phytoplankton species can induce toxin production, for example, in response to an increased predation risk. Compared to the modelled scenario, inducible toxin production would enhance the evolutionary advantage of the toxic strain and promote its persistence, as it avoids costs when predation is low by down-regulating production of toxins. This may imply that the toxic strain dominates even under reduced grazing pressure (e.g. after local enrichment of toxins, see step 3 above) and thus outcompetes the non-toxic strain in the long term. However, both strains could still coexist if the toxic strain faces maintenance costs (i.e. costs that occur even when toxins are not expressed) or if the induction/down-regulation of toxin production is delayed relative to the changes in grazing pressure [27].

Phytoplankton cell division is typically limited by the cell-internal nutrient content [28] rather than the local external concentration as in our model. Including a nutrient storage of phytoplankton cells would allow for cell division even in temporal absence of external nutrients. This may lead to larger cell patches as local competition that counteracts cell clustering is reduced. At first sight, larger patches promote toxic cells sharing their public good with more conspecifics. However, it also increases the chance that non-toxic cells randomly enter patches of toxic cells and outcompete them in the long term. Hence, the frequency of toxic strains in nature likely depends on the degree of local competition, originating from nutrient and light limitation (under dense bloom conditions) and shaped by nutrient storage capacities.

In line with our results (figure 1*c*), several empirical studies have revealed a so-called 'mosaic structure' of toxin concentration within waterbodies, although sampled on a broader spatial scale of ten to several hundred metres [29–31]. Patchiness of phytoplankton cells also occurs on a finer scale down to centimetres [32,33] and we argue that this must hold also for the produced toxins. Previous research suggested that this mosaic structure originates from abiotic drivers [34] or highlighted varying ratios of toxic and non-toxic strains [2,35]. Our study shows for the first time that the spatial heterogeneity in toxin concentration may simply rely on demographic processes generating distinct patches of toxic and non-toxic strains on a microscale (figure 1*c*). Future studies may sample toxic phytoplankton on a finer spatial resolution to provide more empirical insights on patchiness.

In oceans and lakes, many processes affect phytoplankton patchiness on the micro- and macroscale, including abiotic (e.g. nutrient, light or temperature gradients) and biotic ones (e.g. vertical migration, grazing) [17]. Only some of them have the potential to create the critical spatial separation of phytoplankton strains/species needed for the evolution of toxins as a public good. For example, motile phytoplankton may become patched [33] and spatially separated from non-motile phytoplankton in certain turbulent environments [36], or buoyant cyanobacteria distance themselves from sinking or neutrally buoyant cells on a vertical scale, depending on mixing properties [37]. Hence, in contrast to the diffusive motility considered in our model, directional motility (e.g. vertical migration or buoyancy) may promote spatial

heterogeneity even under high turbulence and may play an important role in the success of toxic phytoplankton. Colony formation represents another source for clonal patchiness, e.g. in cyanobacteria.

Patchiness depends on random cell motility. For dinoflagellates, typical cell diffusivities D_C range from 10^{-5} to $10^{-4}\,\mathrm{cm^2\,s^{-1}}$ [38], corresponding to swimming speeds around $100\,\mu\mathrm{m\,s^{-1}}$. At such a high D_C, patchiness cannot be maintained and toxic cells go extinct in the simulations (figure 2). Decreasing D_C below $10^{-5}\,\mathrm{cm^2\,s^{-1}}$ enables the survival of the toxic strain. Very high densities of toxic cells are reached between 10^{-7} and $10^{-6}\,\mathrm{cm^2\,s^{-1}}$ (figure 2), which is the typical diffusivity range of cyanobacteria and toxic haptophytes [38]. Therefore, our proposed mechanism may be more relevant for slowly moving or non-motile phytoplankton species, like toxic haptophytes and *Pseudo-Nitzschia* spp. diatoms, or for species with collective directional movement that does not counteract patchiness like buoyancy or vertical migration. For example, dinoflagellate cells may simultaneously migrate to other water depths, which would maintain patches of toxic cells with elevated toxin concentrations despite high motility [39].

The evolution of toxins as a public good may depend not only on the motility of the phytoplankton cells, but, in case of toxins functioning as defense, also on predator traits (e.g. motility, selectivity or ability to sense toxins). To keep our model general and simple, we did not consider an explicit zooplankton predator. Future studies may survey how certain predator species affect the dynamics.

We assumed that toxin production reduces the cell division rate, as recently found for the dinoflagellate *Alexandrium catenella* [40]. Depending on the phytoplankton species, costs may come in different ways, e.g. with respect to mixotrophy [41] or light competition [42]. In general, empirical evidences for costs of toxin production are rare, and experimental studies have often been unable to demonstrate any measurable direct costs [43,44] or even found that toxic cells can grow faster [45]. Nevertheless, we argue that toxin producers must bear some costs—or else they would be 'Darwinian Demons' that outcompete all non-toxic strains (figure 2*d*), which is not the case in nature. These costs may only emerge in a certain ecological context, making them hard to measure [45]. Our study indicates that costs should be small to allow for toxin evolution, which further complicates the proof of their existence.

Extracellular toxins occur in many different phytoplankton groups [6,14,46,47] and seem to be very labile in water [14,47,48]. This matches our predictions: released toxins should decay fast in order to prevent the spreading of the benefit to non-toxic competitors in neighbouring patches. By contrast, some intracellular toxins appear to be much more stable [14], which would reduce the toxin production effort without promoting competitors.

Cyanobacteria likely evolved toxins before grazers existed [49] and several private goods have been suggested to explain cyanotoxin production, like resistance against oxidative stress [8]. Nevertheless, our proposed mechanism may affect ongoing microevolutionary dynamics even in cyanobacteria as cyanotoxins have been shown to inhibit feeding of grazers like *Daphnia* [50,51]. *Daphnia* can actively avoid toxic patches [52], but cannot pick single edible prey individuals within a patch of bad quality. This behaviour makes even intracellular toxins acting as a public good and significantly lowers grazer density in patches of high toxin concentration [31]. Toxic cyanobacterial strains can indeed invade a population dominated by non-toxic strains [53] and *vice versa* [26], depending on grazing pressure. These strain dynamics are likely affected by horizontal transfer and loss of genes related to toxin production [49].

Toxic dinoflagellates are prevalent in marine systems with copepods as dominant grazers, which feed highly selectively and may render patchiness of toxic cells redundant, especially in case of intracellular toxins. Thus, it seems reasonable that dinoflagellates with intracellular toxins show a high motility, given its advantages regarding other needs (e.g. resource uptake). In contrast, the marine diatom *Pseudo-nitzschia* spp. is non-motile and releases toxins that locally reduce grazing activity by krill [46]. Here, patchiness is beneficial and, indeed, these diatoms cluster in thin subsurface layers [23]. Similarly, our results may also apply to toxic haptophytes like *Prymnesium parvum*, given their low motility and mainly extracellular toxins that act, among others, as a defense against predation [54]. To generalize, the proposed mechanism may be relevant to all kinds of asexually reproducing, toxic organisms with high patchiness (e.g. benthic algae).

Although we focused on toxins reducing grazing, our results may also apply to toxins inhibiting growth or lysing cells of competing algae (i.e. allelochemicals) as indicated by Károlyi *et al.* [55] with a structural similar model, although toxins were not explicitly implemented. A crucial difference between grazer toxins and allelochemicals lies in the properties of their targets. Predators may have a relatively high motility and may actively search for prey organisms. By contrast, toxin-sensitive phytoplankton organisms have a lower motility, which likely reduces their risk of encountering toxic patches. Once they have encountered a toxic patch, however, the toxic effect on them may be more persistent, given their presumed lower ability to actively avoid toxic patches. These behavioural characteristics of the target organisms likely impact the fitness of the toxic phytoplankton and its evolutionary success.

In conclusion, small-scale clonal patchiness, generated by phytoplankton cell division, provides a potential key for the evolution of toxins as a public good and the success of toxic phytoplankton on the community level. Furthermore, it allows for stable coexistence of toxic and non-toxic strains and can explain the frequently observed high genetic diversity in toxic phytoplankton blooms as well as spatial variation in toxin concentration. The cell division-induced patchiness vanishes under high diffusive motility (or high turbulence). Therefore, we conclude that the proposed mechanism applies particularly to toxic phytoplankton with low random motility, like haptophytes, diatoms or cyanobacteria. In general, we emphasize that considering spatial structures of plankton populations can greatly enhance our understanding of evolutionary processes and community dynamics in plankton.

Data accessibility. The paper does not include empirical data. Details on model parameters and additional model results are provided in electronic supplementary material [56].

Authors' contributions. E.E.: conceptualization, formal analysis, funding acquisition, investigation, methodology, software, visualization, writing—original draft, writing—review and editing; U.H.T.: conceptualization, methodology, writing—review and editing; T.K.: conceptualization, funding acquisition, investigation, supervision, writing—review and editing.

All authors gave final approval for publication and agreed to be held accountable for the work performed therein.

Conflict of interest declaration. We declare we have no competing interests.

Funding. Elias Ehrlich was funded by the German Research Foundation (GA 401/24-1, GA 401/26-2) and during the revision process by the EU and the federal state of Mecklenburg-Vorpommern, Germany (MV-I.18-LM-004, B730117000069). The Centre for Ocean Life is supported by the Villum Foundation.

Acknowledgements. We thank two anonymous reviewers for helpful comments on an earlier draft of the manuscript.

References

1. Hallegraeff GM. 1993 A review of harmful algal blooms and their apparent global increase. *Phycologia* **32**, 79–99. (doi:10.2216/i0031-8884-32-2-79.1)
2. Carrillo E, Ferrero LM, Alonso-Andicoberry C, Basanta A, Martín A, López-Rodas V, Costas E. 2003 Interstrain variability in toxin production in populations of the cyanobacterium *Microcystis aeruginosa* from water-supply reservoirs of Andalusia and lagoons of Doñana National Park (southern Spain). *Phycologia* **42**, 269–274. (doi:10.2216/i0031-8884-42-3-269.1)
3. Cusick KD, Widder EA. 2020 Bioluminescence and toxicity as driving factors in harmful algal blooms: ecological functions and genetic variability. *Harmful Algae* **98**, 101850. (doi:10.1016/j.hal.2020.101850)
4. Driscoll WW, Hackett JD, Ferrière R. 2016 Eco-evolutionary feedbacks between private and public goods: evidence from toxic algal blooms. *Ecol. Lett.* **19**, 81–97. (doi:10.1111/ele.12533)
5. Long M, Marie D, Szymczak J, Toullec J, Bigeard E, Sourisseau M, Le Gac M, Guillou L, Jauzein C. 2021 Dinophyceae can use exudates as weapons against the parasite *Amoebophrya* sp. (Syndiniales). *ISME Commun.* **1**, 34. (doi:10.1038/s43705-021-00035-x)
6. Nielsen LT, Krock B, Hansen PJ. 2013 Production and excretion of okadaic acid, pectenotoxin-2 and a novel dinophysistoxin from the DSP-causing marine dinoflagellate *Dinophysis acuta* – effects of light, food availability and growth phase. *Harmful Algae* **23**, 34–45. (doi:10.1016/j.hal.2012.12.004)
7. Glibert PM, Wilkerson FP, Dugdale RC, Raven JA, Dupont CL, Leavitt PR, Parker AE, Burkholder JM, Kana TM. 2016 Pluses and minuses of ammonium and nitrate uptake and assimilation by phytoplankton and implications for productivity and community composition, with emphasis on nitrogen-enriched conditions. *Limnol. Oceanogr.* **61**, 165–197. (doi:10.1002/lno.10203)
8. Dittmann E, Kehr J. 2013 Cyanobakterielle Toxine – von der Biosynthese zur Funktion. *BIOspektrum* **19**, 16–18. (doi:10.1007/s12268-013-0262-8)
9. Xu J, Hansen PJ, Nielsen LT, Krock B, Tillmann U, Kiørboe T. 2017 Distinctly different behavioral responses of a copepod, *Temora longicornis*, to different strains of toxic dinoflagellates, *Alexandrium* spp. *Harmful Algae* **62**, 1–9. (doi:10.1016/j.hal.2016.11.020)
10. Driscoll WW, Pepper JW. 2010 Theory for the evolution of diffusible external goods. *Evolution* **64**, 2682–2687. (doi:10.1111/j.1558-5646.2010.01002.x)
11. Cheng HH. 1995 Characterization of the mechanisms of allelopathy. In *Allelopathy: organisms, processes and applications* (eds Inderjit, KMM Dakshini, FA Einhellig), pp. 132–141. Washington, DC: American Chemical Society.
12. Lewis WM. 1986 Evolutionary interpretations of allelochemical interactions in phytoplankton algae. *Am. Nat.* **127**, 184–194. (doi:10.1086/284477)
13. Drescher K, Nadell CD, Stone HA, Wingreen NS, Bassler BL. 2014 Solutions to the public goods dilemma in bacterial biofilms. *Curr. Biol.* **24**, 50–55. (doi:10.1016/j.cub.2013.10.030)
14. Blossom HE, Andersen NG, Rasmussen SA, Hansen PJ. 2014 Stability of the intra- and extracellular toxins of *Prymnesium parvum* using a microalgal bioassay. *Harmful Algae* **32**, 11–21. (doi:10.1016/j.hal.2013.11.006)
15. Nowak MA. 2006 Five rules for the evolution of cooperation. *Science* **314**, 1560–1563. (doi:10.1126/science.1133755)
16. Bainbridge R. 1957 The size, shape and density of marine phytoplankton concentrations. *Biol. Rev.* **32**, 91–115. (doi:10.1111/j.1469-185X.1957.tb01577.x)
17. Pinel-Alloul B, Ghadouani A. 2007 Spatial heterogeneity of planktonic microorganisms in aquatic systems. In *The spatial distribution of microbes in the environment* (eds R Franklin, A Mills), pp. 201–307. New York, NY: Springer.
18. Young WR, Roberts AJ, Stuhne G. 2001 Reproductive pair correlations and the clustering of organisms. *Nature* **412**, 328–331. (doi:10.1038/35085561)
19. Lloyd M. 1967 'Mean crowding'. *J. Anim. Ecol.* **36**, 1. (doi:10.2307/3012)
20. Jonsson PR, Pavia H, Toth G. 2009 Formation of harmful algal blooms cannot be explained by allelopathic interactions. *Proc. Natl Acad. Sci. USA* **106**, 11 177–11 182. (doi:10.1073/pnas.0900964106)
21. Franks PJS, Inman BG, MacKinnon JA, Alford MH, Waterhouse AF. 2021 Oceanic turbulence from a planktonic perspective. *Limnol. Oceanogr.* **67**, 348–363. (doi:10.1002/lno.11996)
22. Wüest A, Lorke A. 2003 Small-scale hydrodynamics in lakes. *Annu. Rev. Fluid Mech.* **35**, 373–412. (doi:10.1146/annurev.fluid.35.101101.161220)
23. Rines J, Donaghay P, Dekshenieks M, Sullivan J, Twardowski M. 2002 Thin layers and camouflage: hidden *Pseudo-nitzschia* spp. (Bacillariophyceae) populations in a fjord in the San Juan Islands, Washington. *Mar. Ecol. Prog. Ser.* **225**, 123–137. (doi:10.3354/meps225123)
24. Durham WM, Stocker R. 2012 Thin phytoplankton layers: characteristics, mechanisms, and consequences. *Annu. Rev. Mar. Sci.* **4**, 177–207. (doi:10.1146/annurev-marine-120710-100957)
25. Alpermann TJ, Tillmann U, Beszteri B, Cembella AD, John U. 2010 Phenotypic variation and genotypic diversity in a planktonic population of the toxigenic marine dinoflagellate *Alexandrium tamarense* (Dinophyceae). *J. Phycol.* **46**, 18–32. (doi:10.1111/j.1529-8817.2009.00767.x)
26. Briand E, Escoffier N, Straub C, Sabart M, Quiblier C, Humbert JF. 2009 Spatiotemporal changes in the genetic diversity of a bloom-forming *Microcystis aeruginosa* (cyanobacteria) population. *ISME J.* **3**, 419–429. (doi:10.1038/ismej.2008.121)
27. Selander E, Fagerberg T, Wohlrab S, Pavia H. 2012 Fight and flight in dinoflagellates? Kinetics of simultaneous grazer-induced responses in *Alexandrium tamarense*. *Limnol. Oceanogr.* **57**, 58–64. (doi:10.4319/lo.2012.57.1.0058)
28. Droop MR. 1973 Some thoughts on nutrient limitation in algae. *J. Phycol.* **9**, 264–272. (doi:10.1111/j.1529-8817.1973.tb04092.x)
29. Carmichael WW, Gorham PR. 1981 The mosaic nature of toxic blooms of cyanobacteria. In *The water environment: algal toxins and health* (ed. WW Carmichael), pp. 161–172. New York, NY: Plenum Press. (doi:10.1007/978-1-4613-3267-1)
30. Srivastava VC, Choi AR, Kim W, Lee JA. 1999 Horizontal and vertical distribution of protein phosphatase inhibitors of microcystin class in the Naktong river, Korea. *Algae* **14**, 67–72.
31. Reichwaldt ES, Song H, Ghadouani A. 2013 Effects of the distribution of a toxic microcystis bloom on the small scale patchiness of zooplankton. *PLoS ONE* **8**, e66674. (doi:10.1371/journal.pone.0066674)
32. Waters R, Mitchell J, Seymour J. 2003 Geostatistical characterisation of centimetre-scale spatial structure of *in vivo* fluorescence. *Mar. Ecol. Prog. Ser.* **251**, 49–58. (doi:10.3354/meps251049)
33. Breier RE, Lalescu CC, Waas D, Wilczek M, Mazza MG. 2018 Emergence of phytoplankton patchiness at small scales in mild turbulence. *Proc. Natl Acad. Sci. USA* **115**, 12 112–12 117. (doi:10.1073/pnas.1808711115)
34. Kaebernick M, Neilan BA. 2001 Ecological and molecular investigations of cyanotoxin production. *FEMS Microbiol. Ecol.* **35**, 1–9. (doi:10.1016/S0168-6496(00)00093-3)
35. Vezie C, Brient L, Sivonen K, Bertru G, Lefeuvre JC, Salkinoja-Salonen M. 1998 Variation of microcystin content of cyanobacterial blooms and isolated strains in Lake Grand-Lieu (France). *Microb. Ecol.* **35**, 126–135. (doi:10.1007/s002489900067)
36. Durham WM, Climent E, Barry M, De Lillo F, Boffetta G, Cencini M, Stocker R. 2013 Turbulence drives microscale patches of motile phytoplankton. *Nat. Commun.* **4**, 2148. (doi:10.1038/ncomms3148)
37. Huisman J, Sharples J, Stroom JM, Visser PM, Kardinaal WEA, Verspagen JMH, Sommeijer B. 2004

Changes in turbulent mixing shift competition for light between phytoplankton species. *Ecology* **85**, 2960–2970. (doi:10.1890/03-0763)

38. Visser AW, Kiørboe T. 2006 Plankton motility patterns and encounter rates. *Oecologia* **148**, 538–546. (doi:10.1007/s00442-006-0385-4)
39. MacIntyre J, Cullen J, Cembella A. 1997 Vertical migration, nutrition and toxicity in the dinoflagellate *Alexandrium tamarense*. *Mar. Ecol. Progr. Ser.* **148**, 201–216. (doi:10.3354/meps148201)
40. Park G, Dam HG. 2021 Cell-growth gene expression reveals a direct fitness cost of grazer-induced toxin production in red tide dinoflagellate prey. *Proc. R. Soc. B* **288**, 20202480. (doi:10.1098/rspb.2020.2480)
41. Blossom HE, Hansen PJ. 2020 The loss of mixotrophy in *Alexandrium pseudogonyaulax:* implications for trade–offs between toxicity, mucus trap production, and phagotrophy. *Limnol. Oceanogr.* **66**, 528–542. (doi:10.1002/lno.11621)
42. Kardinaal WEA, Tonk L, Janse I, Hol S, Slot P, Huisman J, Visser PM. 2007 Competition for light between toxic and nontoxic strains of the harmful cyanobacterium *Microcystis*. *Appl. Environ. Microbiol.* **73**, 2939–2946. (doi:10.1128/AEM.02892-06)
43. John EH, Flynn KJ. 2000 Growth dynamics and toxicity of *Alexandrium fundyense* (Dinophyceae): the effect of changing N:P supply ratios on internal toxin and nutrient levels. *Eur. J. Phycol.* **35**, 11–23. (doi:10.1080/09670260010001735581)
44. Selander E, Cervin G, Pavia H. 2008 Effects of nitrate and phosphate on grazer-induced toxin production in *Alexandrium minutum*. *Limnol. Oceanogr.* **53**, 523–530. (doi:10.4319/lo.2008.53.2.0523)
45. Ryderheim F, Selander E, Kiørboe T. 2021 Predator-induced defence in a dinoflagellate generates benefits without direct costs. *ISME J.* **15**, 2107–2116. (doi:10.1038/s41396-021-00908-y)
46. Bargu S, Lefebvre K, Silver M. 2006 Effect of dissolved domoic acid on the grazing rate of krill *Euphasia pacifica*. *Mar. Ecol. Progr. Ser.* **312**, 169–175. (doi:10.3354/meps312169)
47. Chiswell RK, Shaw GR, Eaglesham G, Smith MJ, Norris RL, Seawright AA, Moore MR. 1999 Stability of cylindrospermopsin, the toxin from the cyanobacterium, *Cylindrospermopsis raciborskii*: effect of pH, temperature, and sunlight on decomposition. *Environ. Toxicol.* **14**, 155–161. (doi:10.1002/(SICI)1522-7278(199902)14:1<155::AID-TOX20>3.0.CO;2-Z)
48. Hansen PJ. 1989 The red tide dinoflagellate *Alexandrium tamarense*: effects on behaviour and growth of a tintinnid ciliate. *Mar. Ecol. Progr. Ser.* **53**, 105–116. (doi:10.3354/meps053105)
49. Rantala A, Fewer DP, Hisbergues M, Rouhiainen L, Vaitomaa J, Borner T, Sivonen K. 2004 Phylogenetic evidence for the early evolution of microcystin synthesis. *Proc. Natl Acad. Sci. USA* **101**, 568–573. (doi:10.1073/pnas.0304489101)
50. Agrawal MK, Zitt A, Bagchi D, Weckesser J, Bagchi SN, Von Elert E. 2005 Characterization of proteases in guts of *Daphnia magna* and their inhibition by *Microcystis aeruginosa* PCC 7806. *Environ. Toxicol.* **20**, 314–322. (doi:10.1002/tox.20123)
51. Lukas M, Wacker A. 2014 *Daphnia*'s dilemma: adjustment of carbon budgets in the face of food and cholesterol limitation. *J. Exp. Biol.* **217**, 1079–1086. (doi:10.1242/jeb.094151)
52. Laurén-Määttä C, Kleiven O, Kiviranta J. 1997 Horizontal distribution of *Daphnia pulex* in response to toxic and non-toxic algal extracts. *J. Plankton Res.* **19**, 141–148. (doi:10.1093/plankt/19.1.141)
53. Benndorf J, Henning M. 1989 *Daphnia* and toxic blooms of *Microcystis aeruginosa* in Bautzen Reservoir (GDR). *Int. Rev. der gesamten Hydrobiologie und Hydrographie* **74**, 233–248. (doi:10.1002/iroh.19890740302)
54. Manning SR, La Claire JW. 2010 Prymnesins: toxic metabolites of the golden alga, *Prymnesium parvum* carter (Haptophyta). *Mar. Drugs* **8**, 678–704. (doi:10.3390/md8030678)
55. Károlyi G, Neufeld Z, Scheuring I. 2005 Rock-scissors-paper game in a chaotic flow: the effect of dispersion on the cyclic competition of microorganisms. *J. Theor. Biol.* **236**, 12–20. (doi:10.1016/j.jtbi.2005.02.012)
56. Ehrlich E, Thygesen UH, Kiørboe T. 2022 Evolution of toxins as a public good in phytoplankton. Figshare. (doi:10.6084/m9.figshare.c.6035667)